March 17, 2001 Submitted to Journal of Glaciology

Seasonal and Interannual Variations of Ice Sheet Surface Elevation at the Summit of Greenland: Observed and Modeled

H. Jay Zwally,

Ocean and Ice Branch Code 971, NASA/Goddard Space Flight center, Greenbelt, MD 20771, USA

Li Jun,

Raytheon ITSS Code 971, NASA/Goddard Space Flight center, Greenbelt, MD 20771, USA

ABSTRACT

Observed seasonal and interannual variations in the surface elevation over the summit of the Greenland ice sheet are modeled using a new temperature-dependent formulation of firn-densification and observed accumulation variations. The observed elevation variations are derived from ERS-1 and ERS-2 radar altimeter data for the period between April 1992 and April 1999. A multivariate linear/sine function is fitted to an elevation time series constructed from elevation differences measured by radar altimetry at orbital-crossovers. The amplitude of the seasonal elevation cycle is 0.25 m peak-to-peak, with a maximum in winter and a minimum in summer. Inter-annually, the elevation decreases to a minimum in 1995, followed by an increase to 1999, with an overall average increase of 4.2 cm a^{-1} for 1992 to 1999. Our densification formulation uses an initial field-density profile, the AWS surface temperature record, and a temperature-dependent constitutive relation for the densification that is based on laboratory measurements of crystal growth rates. The rate constant and the activation energy commonly used in the Arrhenius-type constitutive relation for firn densification are also temperature dependent, giving a stronger temperature and seasonal amplitudes about 10 times greater than previous densification formulations. Summer temperatures are most important, because of the

strong non-linear dependence on temperature. Much of firn densification and consequent surface lowering occurs within about three months of the summer season, followed by a surface build-up from snow accumulation until spring. Modeled interannual changes of the surface elevation, using the AWS measurements of surface temperature and accumulation and results of atmospheric modeling of precipitation variations, are in good agreement with the altimeter observations. In the model, the surface elevation decreases about 20 cm over the seven years due to more compaction driven by increasing summer temperatures. The minimum elevation in 1995 is driven mainly by a temporary accumulation decrease and secondarily by warmer temperatures. However, the overall elevation increase over the seven years is dominated by the accumulation increase in the later years.

INTRODUCTION

Glaciers and ice sheets continuously adjust their dimensions in response to current and past climatic change. Long term ($>10^3$ yr) changes of the surface elevation are primarily due to changes in ice dynamics reflecting past mass balance states of the ice sheet. Short term (decadal) or seasonal changes are caused by interannual or seasonal variations of weather conditions such as snow accumulation and surface air temperature (e.g. Braithwaite and others, 1994). Changes in surface elevation of polar ice sheets are of great importance to mass balance studies since changes in ice volume may be determined from changes in ice thickness obtained from surveys of changes in surface elevation by satellite altimetry (e.g. Davis et al, 1998; Zwally and Brenner, 2001, Shepherd et al, 2001, and Zwally et al, submitted). Surface elevation changes are equivalent to ice thickness changes minus the vertical motion of the bedrock, which is generally smaller and can be separately estimated. However, short-term changes caused by variations in rates of near-surface firn compaction must also be accounted for (Arthern and Wingham, 1998).

In dry-snow zones, seasonal and interannual changes in surface elevation may be caused by variations in the rates of accumulation and firn densification. The rate of densification is also be affected by surface temperature and rate of accumulation. Field observations in west Greenland show that variations of near-surface firn density can cause annual surface elevation changes of the order of ± 0.1-0.2 m (Braithwaite and others 1994). McConnell and others (2000) have recently modeled accumulation rates based on data from 11 ice cores located near the 2000-m contour of the Greenland ice sheet. They suggest that the ice sheet elevation varies by tens of centimeters from year to year simply because of changing snow accumulation.

Ice sheet surface elevations derived from satellite radar altimetry have exhibited seasonal variations (Zwally and others, 1989 and Yi and others, 1997), but their specific cause in dry snow zones has been uncertain (Yi and others, 1997). In percolation areas of Greenland, an observed seasonal cycle with a maximum in mid-April just before the melt season and a minimum in mid-October is consistent with a lowering caused by summer melting and firn compaction (Zwally and Brenner, 2001). Also, the observed elevations in the ablation zones show similar summer minimum that can be associated with summer melting. However, in the dry snow zones an observed amplitude of several tens of centimeters, with a minimum typically occurring in summer, is generally larger than expected from seasonal variations in snowfall alone. Other potential causes for seasonal variations in Geosat altimetry data discussed by Yi and others, 1997 include unresolved satellite orbit errors, variations in the subsurface versus surface radar backscatter, and variations in firn densification. However, examination of ERS orbit quality over oceans eliminates orbit errors as a cause. Also, the observed seasonal cycle with a winter maximum are not explained by seasonal variations in the effective radar-backscatter depth. If anything, fresher fine-grained winter snow might have more radar penetration and cause detection of a lower surface, giving a winter minimum in contradiction to the observations. Furthermore, calculations of a seasonal cycle in firn compaction using a densification model and similar to Herron and Langway or Arthern and Wingham (1998) give small seasonal amplitudes of only a few centimeters (M. Spencer and R. Alley, Pers. Com.).

The temperature dependence of densification rate from the constitutive relation used in previous models is based on the Arrhenius equation, with an exponential function of both activation energy and temperature, and a multiplicative (rate-constant) that is either independent of or weakly dependent on temperature. Although the Arrhenius formulation is widely used to describe various processes in snow and ice, including deformation (Paterson, 1994) and grain growth (e.g. Gow, 1969), different values of the activation-energy "constant" are typically used for different processes or for different regimes of the same process. For example, Herron and Langway (1980) used different rate constants and activation energies for density less than or greater than 0.55 in their densification model. Arthern and Wingham, 1998 used different formulations and constants at different depths in their densification model to describe the dominate deformation processes such as grain-boundary sliding (e. g. Alley, 1987) or dislocation creep (Wilkenson and Ashby, 1975). The relevant parameters were determined by fitting field-density profiles assuming constant accumulation rate and temperature under steady state assumption (Herron and Langway 1980; Alley 1987). However, this is not the case in practice. Snow precipitation varies in time and temperatures in upper firn layers vary greatly during the year causing large variations of snow density as observed in field measurements (e.g. Koerner, 1971, Gow 1968, Qin and others 1988, Han and Yang 1988, Alley 1987, Gerland and others 1999).

In our model, we take into account the seasonal cycle of temperature in the upper firn layers, which is important firstly because of the non-linear dependence of temperature even in the standard Arrhenius-type formulation. More importantly, however, we use a temperature-dependent activation energy and a temperature-dependent rate constant based on the crystal growth studies of Jacka and Li (1994). Using the detailed records of accumulation and temperature from AWS for the summit in Greenland, and atmospheric model results on precipitation variations (Bromwich et al, in press), we model the densification rates in top 15 m of firn and obtain elevation changes for comparison with the satellite altimeter measurements. Our reference location for this study is 72° 34' N, 38° 27' W, which is the approximate location of GISP2 and the AWS about 25 km west

of the actual elevation summit. The radar altimeter measurements are averaged of area of 200 km diameter around this point.

SURFACE CONDITIONS

A continuous surface air temperature record for the Greenland summit region from 1987 -1999 has been constructed by Shuman and others (1999). His record is a composite of data from three automatic weather stations (AWS) since 1995 and satellite passive microwave data from the same locations. The surface air temperatures over the period of April 1992 to April 1999 (Figure 1) show an average seasonal of about 38 °C (mean amplitude) with a mean temperature of about -30 °C. Both mean summer (June to August) and mean annual temperatures show a general increasing trend and an interannual variability about 5 °C with a minimum in 1992 and maximum in 1995.

Snow accumulation data has been collected from AWS for the summit of Greenland between May 1995 and August 1998 using the sonic technique (Steffen and others 1999). This technique measures the distance between the snow surface and a sonic sensor mounted on the AWS tower. Decreases in distance are caused mainly by snow accumulation (snow fall and drift) and increases in distance by evaporation and wind erosion. The regression line through the measured distance versus time gives a surface rise of 0.625 m a^{-1}, which must be multiplied by the near-surface firn density to get accumulation rate. Integrating the firn density profile to a depth of the firn added in one year (.625 m) gives an average firn density of 0.400, compared to a surface density of 0.332, and an annual accumulation rate of 250 kg m^{-2}. The density estimate attempts to account for the effect of new-snow compaction for an AWS pole tower inserted a few meters in the firn. The accumulation rate obtained is slightly higher in comparison with 220 kg m^{-2} a^{-1} from Ohmura and Reeh, (1991). The derived accumulation rate from AWS in Figure 1 shows two sudden increases of snow surface height in July 1995 and July 1997 caused by large snow storms. The surface increases are approximate 0.4 and 0.2 m respectively.

By using the improved dynamic atmosphere model, Bromwich and others (in press) recently re-evaluated the precipitation-evaporation (P-E) distribution and its interannual changes over the period of 1985-1999 for the Greenland ice sheet. A pronounced downward trend in annual precipitation from 1985-1995 followed by a marked increase from 1995-1999 was found. However, for the same period their modeling results for Summit of Greenland seem 50% less in comparison with AWS measurements from the field. This may indicate that a scaling factor should be used in the model to allow such comparison between the measured accumulation and model-retrieved precipitation. Similar to the treatment (departure from mean divided by mean) from Bromwich and others (submitted) we normalize their modeled snow precipitation for the summit of Greenland by using the mean accumulation rate (250 kg m^{-2} a^{-1}) derived from AWS measurements over the period between April 1992 and April 1999 as shown in Figure 1. Interestingly, the modeled precipitation also shows peaks in the summers of 1995 an 1997 corresponding to the storms observed in the AWS data, albeit with smaller amplitude.

The summit region of Greenland ice sheet is in the dry snow zone due to its negligible summer melting (Benson 1962). The density profile Gow (1997) for the summit region shows a firn-ice transition depth around 75-77 m where the firn density reaches approximate 830 kg m^{-3}. During May 1987, a number of shallow cores (to approximately 17 m depth) were recovered over a 150 x 150 km survey grid in Central Greenland. Detailed density measurements were made in depth intervals less than 0.1 m (Bolzan and Strobel, 1994). The regression line through the data from 8 cores gives a surface snow density of 332 kg m^{-3}, increasing to 550 kg m^{-3} by 15 m depth.

SURFACE H(t) FROM RADAR ALTIMETRY DATA

The observed elevation variations are derived from ERS-1 and ERS-2 radar altimeter data for the period between April 1992 and April 1999. Elevation changes are derived from surface elevation differences, $dH_{21} = H_2 - H_1$, measured at crossover locations where sub-

satellite paths intersect at successive times t_2 and t_1. Sets of N values of $(dH_{21})_i$ are averaged over selected areas to reduce the error of the mean. Time-series of surface elevations, H(t), having sufficient resolution to show seasonal changes are created by the sequence of average crossover differences between the first 90-day interval and each of the successive 90-day intervals, combined with the sequence from the second interval crossed with each successive interval, and so forth for the sequences for the third and greater intervals (Zwally and Brenner, 2001). Typically, crossovers within a 100 km radius and ± 250 m elevation of the central point are included. The data are also corrected for an unexpected inter-satellite bias that was determined by Brenner and others (2000) from analysis of crossover differences acquired during the 12 months of overlapping operation of ERS-1 and ERS-2. At Summit, the bias lowers ERS-2 elevations by 10.6 cm relative to ERS-1. A multivariate linear/sine function is then fitted to the H(t) series giving a linear trend, amplitude of the seasonal cycle in the data, and its phase.

The H(t) elevation series for the Summit vicinity for the period April 1992 to April 1999 is shown in Figure 1 with the fitted linear trend and seasonal cycle. The regression line shows that the winter snow surface is higher than summer with an average amplitude of 0.25 m peak to peak and a minimum in mid-July. The average increase of the surface height is 4.2 cm a^{-1} during this period. Note that a significant (≈ 0.5m) downward trend in the surface elevation occurs between 1992 and 1995, followed by the pronounced increase from 1995 to 1999.

SURFACE-ELEVATION MODEL

Regime of surface elevation change

The elevation change of the ice sheet snow surface is the consequence of a combination of several vertical velocities components illustrated in Figure 2. Snow accumulation increases the surface height at the rate $A(t)/\rho_0$, while firn compaction, ice flow and surface ablation generate velocities that reduce the surface height, according to

$$dH(t)/dt = A(t)/\rho_0 - V_{fc}(t) - V_{ice} - B(t) \quad (1)$$

where $dH(t)/dt$ is the change in snow surface elevation (H), A(t) is the accumulation rate, and ρ_0 is firn density at the surface (300 kg m^{-3}). V_{fc} (t), V_{ice} , and B(t) are the vertical velocity of the surface due to firn compaction, ice flow and surface ablation respectively. All components in equation (1) are usually a function of time (t), but V_{ice} changes on time scales much longer than the seasonal changes of the other components. At steady state, $V_{ice} = A/\rho_i$, where <A> is annual mean accumulation rate (independent of time), where ρ_i is the density of solid ice (917 kg m^{-3}). Since the Summit of Greenland is in the dry snow zone, B(t) is neglected in the present analysis. The variations of the surface height with time, H(t), on seasonal to interannual time scales are thus determined by the rates of snow accumulation and densification.

A multi-layer system

The densification rate at a depth in dry snow zone is determined by the overlying pressure, firn temperature, and highly dependent on firn density (cf. Shapior 1997, Bader 1962). Therefore, the present surface height change due to firn densification also relies on the densification history by way of the existing firn density profile. To assess such change for the Summit of Greenland, a multi-layer numerical model is developed. We consider that the total surface height change results from two parts of firn densification: existing firn below the initial surface (at a date considered) and the subsequently precipitated snow (additional accumulation). To calculate the initial surface change with time, we use field density profile (Bolzan and Strobel, 1994) from 0 - 15 m and divide it into multi-layers with initial thickness 0.1 m. Therefore, near the surface each layer in the model corresponds to about 1/7 of the annual deposition. Assuming the density within each layer is reasonably uniform, the change (v_{ij}) of the layer thickness (h_{ij}) caused by the density change at a given depth i and time j (for one time step) is given by

$$v_{ij} = h_{ij}/\rho_{ij} \, (d\rho/dt)_{ij} \quad (2)$$

We consider densification in the firn layer between 0- 15 m as the seasonal variation part, because of seasonal variations of firn temperature in this depth range, and below 15 m as the non-seasonal variation part. Under the steady state assumption, the mass flux through any firn depth per year equals the annual accumulation rate. The total vertical velocity V_{fc} due to any firn densification below depth **z** can be determined by

$$V_{fc}(z) = (\rho_i/\rho(z) - 1) V_{ice} \tag{3}$$

Equation (3) is used to estimate the total vertical velocity due to firn compaction below 15 m.

The vertical velocity from additional accumulation is initially upward by $A(t)/\rho_0$ for the precipitation on a individual day, followed by a decrease on subsequent days as the new precipitation compresses. The vertical velocity due to the densification of the additional snow accumulation (V^1_{fc}) is also computed from equation (2). In this case, h_{ij} is the thickness of the amount of the snow precipitated at each unit of time (t) in days, and one model layer is assigned for each day. The total amount of the surface height change per day can therefore be estimated by

$$\frac{\Delta H(t)}{\Delta t} = \frac{A(t)}{\rho_0} - \sum_{t=1}^{t} V^1_{fc} - \sum_{n=1}^{N} V_{fc}(z) - V_{fc}(z_1) - \frac{\langle A \rangle}{\rho_i} \tag{4}$$

where <A> is the annual mean accumulation rate, N is the number of the divided layers for the firn below the initial surface. Z_1 is the depth at the layer N, which is initially 15 m and then moves downward with time.

Calculation of densification rate

Crucial to all analysis is the densification law for firn, that is a constitutive equation that governs the relation between densification rate ($d\rho/dt$) and physical variables such as temperature and the stress. Based on the assumption that in the densification of firn the proportional change in air gap is proportional to the change in stress due to the weight of overlying snow (Schytt 1958), Herron and Langway (1980) derived an empirical equation as:

$$d\rho/dt = K A^{\alpha} (\rho_i - \rho) \quad (5)$$

where k is a rate constant solely dependent on temperature, A is the mean accumulation rate and exponent α is a constant dependent on the densification mechanisms. The temperature dependence of k follows Arrhenius type relation (Equation 6). Using data collected from 17 sites in Greenland and Antarctica the value of α was found approximately equals 1 for density less than 0.55. By considering the process of grain-boundary sliding, Alley (1987) arrived at an essentially similar relation for the firn deeper than 2 m, which has minimal disturbance from surface weather conditions. However for near surface snow, equation (5) seems to fit field data more closely and also has the advantage of simplicity. In this analysis, we apply equation (5) to each layer of firn to derive the change of the density, and therefore the thickness of the layer, driven by accumulation rate and firn temperature.

Activation energy

Similar to ice creep and grain growth the temperature dependence of densification rate also follows Arrhenius relation shown by

$$K(T) = K_0(T)\exp(-E(T)/RT) \quad (6)$$

In equation (6), both K_0 and activation energy E have usually been taken to be constants independent of temperature. However, for the snow with different densities, Bader

(1962) found E varies from 41.8 to 100.4 kJ mol^{-1}. Herron and Langway (1980) empirically derived average values of E from 10.16 to 21.4 kJ mol^{-1} for the densities below and above 550 kg m^{-3}. Alley (1987) obtained 41 kJ mol^{-1} from his modeled density profiles for four sites in Antarctica, which is rather close to the value often used for grain growth (42 kJ mol^{-1}, Paterson 1994). However, previous studies on ice creep and grain growth (e.g. Barnes and others 1971, Budd and Jacka 1989) suggested that activation energy actually is a function of temperature. Based on grain growth and ice creep rates data, Jacka and Li (1994) examined activation energies for grain growth and ice creep by applying Equation (6) to each small increment of the temperature. They found that E increased significantly with temperature, especially at temperatures above – 10 °C (Figure 3a). The values of E for grain growth and ice creep were similar.

In Equation (6), increasing values of E with increasing temperature will reduce the value of the rate K with temperature, if K_0 is taken to be a constant. However, this is in marked contradiction to the measurements of K(T) that show a strong increase in K with temperature (Jacka and Li, 1994). For K to increase with increasing temperature, the factor K_0 in Eq. 6 must also be strongly temperature dependent. Using the rate data given by Jacka and Li (1994, Table 2), we derived the K_0 (T) shown in Figure 3b from the measured K(T) for grain growth. Therefore, knowing the dependence of both K_0 and E on temperature, K(T) can be calculated according Equation (6). An alternative and equivalent formulation of K(T), following the procedures used by Jacka and Li (1994) to obtain E(T), is given by

$$K(T) = c_0 \exp\left(\frac{-1}{R} \int_{1/T_0}^{1/T} E\left(\frac{1}{T}\right)\, d\frac{1}{T} \right) \tag{7}$$

where c_0 is a constant equal to the value of K at temperature T_0. This formulation implicitly contains the same temperature dependence shown by E(T) and K_0 (T) in Eq. 6. We use Eq. 7 in our densification model and a best fit curve through the data of activation energy given by Jacka and Li (1994) in Figure 3a. For the value of c_0, we use 0.025 and

T_0 = -30 °C that gives K = 0.025 at T = -30 °C (annual mean temperature for the summit), which is a value of K that is between the value of 0.072 for densities < 0.55 and the value of 0.014 for densities > 0.55 obtained at -30° C by Herron and Langway (1980, Eqs. 6a,b). This choice of c_0 also gives a modeled amplitude of 20 cm peak-to-peak for the seasonal variation of surface height, which is close to the mean amplitude shown in the radar altimetry measurements. Although we exercise some selectivity in our choice of c_0 to match the observed seasonal amplitudes, it should be emphasized that without the strong temperature dependence in our formulation (i.e. with only exp (E/T) dependence) the modeled seasonal amplitude would only be millimeters to centimeters.

FIRN TEMPERATURE CALCULATION

Wang et al (in prep.) have analyzed firn and ice temperature evolution driven by surface air temperature between 1982-1999 for the summit of Greenland. The temperature analysis follows the standard one dimensional time-dependent heat-transfer equation (Paterson 1994) written by

$$\rho\, c \frac{\partial T}{\partial t} = K\, \nabla^2 T + \left(\frac{dK}{dz} - \rho\, c\, w \right) \frac{\partial T}{\partial z} + f \qquad (8)$$

where ρ is firn density, c is heat capacity, K is thermal conductivity, T is temperature, w is vertical velocity and f is internal heating. For this study, w is computed based on the constant accumulation rate (250 kg m^{-2} a^{-1}) and f is neglected. Figure 4a presents computed firn temperature variations at several selected depths over the period April 1992 –April 1999. We use the results of this analysis for the firn temperatures in the top 15 m. Below 15 m, vertical velocity due to firn densification is calculated based on Equation (3) under the steady-state assumption, and is therefore independent of temperature. The temperature analysis shows that beside the seasonal cycles of firn temperature, significant interannual variations of mean summer (June to August) temperatures occur at various depths. The interannual variability of summer

temperature is greater than 5° C at the surface, diminishing to about 1° C at 10-15 m, as shown in Figure 4b. The trend in surface summer temperature is positive at 0.3° C a^{-1}, and the trend in mean annual temperature for this period is also positive at 0.4° C a^{-1}.

RESULTS AND DISCUSSION

Seasonal elevation variations for steady state conditions

Figure 5a and b show the modeled seasonal change of the surface elevation densification model, when driven by a steady-state surface air temperature with an annual cycle of amplitude 19° C and annual mean of –30° C and a constant accumulation rate of 250 kg m^{-2} a^{-1}. Also, shown in Figure 5a is the initial surface as it is buried with additional accumulation of snow. The corresponding density variations with depth are shown in Figure 5c. The mean amplitude of the surface height change is 20 cm with the minima occurring in August. Much of firn densification and consequent surface lowering occurs within about two to three months of the late-spring to early-summer season when the upper firn is warmest. The period of maximum firn compaction is followed by a build-up of the surface by snow accumulation during the rest of the year, and the period of buildup is somewhat longer than the period of surface lowering when the compaction is more dominant than accumulation. The enhanced firn compaction driven by summers temperature is most striking in the near surface firn within 1 m, and quickly diminishes with increasing depth as indicated by the initial surface curve in Figure 5a. The seasonality of the compaction rate is reflected in the seasonal variations in the density profile (Figure 5c). The magnitude of the density variations reduces with increasing depth. A similar seasonal density cycle has been observed in high-resolution density measurements made on firn/ice cores in Antarctic (Gerland and others, 1999), and may be reflected in the typically wide scatter of densities in other less detailed density profiles as noted in the introduction.

Interannual elevation variations

Using surface air temperature and accumulation rate data shown in Figure 1a,b as model input, we have examined the surface elevation change due to firn compaction between April 1992 and April 1999 as shown by Figure 6. As shown in Figure 1 for accumulation and Figure 2 for temperature, both of these input data sets that drive the model have significant interannual variations. For comparison, the elevation change from radar altimetry measurements (overlain in Figure 6) closely follows the modeled elevation, although the observations shows several larger spikes. Both curves clearly indicate that snow surface elevation at Summit of Greenland decreased about 0.5 m between 1992 and 1995 followed by a marked increase (0.8 m) with larger annual variations. Along with these general trends, both curves also show significant seasonal peaks, caused by seasonal cycles of the surface temperature in the model.

To separate the effects of temperature and accumulation variations that are input to the model, we compute the elevation change with the observed temperature variations and fixed accumulation rate (curve a) and with the variable accumulation rate and fixed seasonal temperature cycle without out interannual variations (curve b), as shown in (Figure 7). Again, curve a shows the seasonal cycle in surface elevation with the sharp lowering during late spring to early summer. However, it also shows an interannual variability in both the seasonal amplitude (e.g. large during the warmer summer of 1995 shown in Figure 4b and small during the colder summer of 1996) and the general decrease in elevation due increasing trend in temperatures during this period, particularly in summer. About 0.2 m elevation decrease is in response to the increase of the summer temperature during this period.

Curve b in figure 7 shows that variations of accumulation rate play the dominant role in the interannual changes of the surface elevation over this period. The surface elevation decreases between 1992 and 1995, followed by the significant increase in response to the accumulation rate change. Although the decrease from 1992 to 1995 is primarily driven by accumulation, the warmer summer temperature of 1995 also contributes to the minimum shown in both the model and the altimeter observations. Over the 7 years the effect of warmer temperatures lowers the surface by about 3 cm a^{-1}, but the effect of

increased precipitation dominants to bring the overall increase to 4.2 cm a^{-1} as obtained from the multivariate fit to the altimeter data. Supporting information for the variation in accumulation rates is provided by the analysis of shallow ice cores, which shows an anomalously low accumulation in 1995 followed by marked increase in 1996 (Moseley-Thompson et al, in press).

CONCLUSIONS

The agreement between the modeled surface elevation, which is driven by observed temperatures and modeled/observed accumulation variations, and the elevation time-series derived from radar altimetry would seem to confirm the validity of the model and the reality of the observed elevations. The model produces very well the essential features of the altimeter observations, including a seasonal cycle and a marked decrease to 1995 followed by a marked increase. Although interannual temperature variations contribute to the decrease in 1995, the predominant effect is the interannual variation in accumulation that is supported by independent evidence for ice cores. The observed elevation trend for 1992-1999 is 4.2 cm a^{-1}, which is slightly larger than the 3.6 ± 2.1 cm a^{-1} obtained by Hamilton and Whillans (2000) by the GPS coffee-can method at the GISP2 summit and larger than the -3 ± 4 cm a^{-1} by Hvidberg and others (1997) nearer the actual summit about 25 km to the east.

A principal new feature of the model is the stronger temperature dependence of the constitutive relation governing firn densification. This stronger temperature dependence is based on laboratory measurements of rates of grain growth and ice creep. We apply the temperature dependence found in the laboratory measurements to the densification process as well. Firn densification, grain growth, and ice creep are processes that have been previously treated similarly with rates described by the Arrhenius equation.

A principal result of the elevation model is that most of the firn compaction in the upper firn occurs in late spring and early summer when temperatures are warmest. This

seasonal variability in compaction rate is sufficient to cause a cycle in the density profile that is gradually dampened in amplitude as the firn continues to compress with depth. Additional confirmation of the validity of the model derives from the modeled seasonal cycle in density with depth, which was previously observed in Antarctic cores but not explained (Gerland and others, 1999). Although the density data (Bolzan and Strobel, 1994) for the summit have not been analyzed in detail for a seasonal density data, the data are consistent with our model in that the densities appear scattered within a density band about 0.08 wide near the surface (c.f. Fig. 5c), which decreases in width with depth and may contain a seasonal cycle. For example, the profile from J. F. Bolzan (pers. com., 1999 and Fig.4 in Hamilton and Whillans, 2000) shows about 19 alternate higher and lower densities between 2 m and 17 m, which is consistent with an annual cycle assuming that a only few cycles are missed by the sampling ($\approx$ 5 samples per annual layer).

At any time, the rate of densification depends on the temperature and accumulation history, which was simplified in our present model by assuming the firn was in steady state and using a measured mean density profile on the initial day (4/14/1992). However, longer-term temperature and precipitation records can be used to calculate an initial state of temperature and density profile with seasonal variations. Future efforts should also include laboratory measurements of the temperature dependence of firn-densification rates to refine the coefficients used in the rate equation, direct measurements of densification rates versus depth by automated instrumentation placed in the firn, and extension of the elevation model to firn percolation zones and cold, low accumulation regions. Finally, other forcings such as drift and wind compaction to the snow may need to be considered. Strong wind may enhance snow compaction producing higher density firn layers (Goodwin, 1991), while in other cases it also brings in large amounts of low-density snowfall in very short periods causing larger fluctuations of surface height. Some of the departures between modeled and observed results shown in figure 5 may due to such causes.

The effect of interannual variations in densification (caused by changes in temperature, density, and accumulation rate at the surface) on the use of altimeter observations for

studies of mass balance was addressed by (Arthern and Wingham, 1998; Wingham, 2001). While a greater sensitivity to temperature would seem to complicate the interpretation of satellite altimeter data, it may only change the response time to variations in accumulation. Since the response time of the surface elevation to accumulation anomalies is governed in effect by how fast the anomaly moves down the density profile, on average the greater sensitivity to temperature should not make much difference. However, accumulation anomalies that occur during the warmer seasons when near-surface densification is faster should persists for a shorter time than anomalies occurring during the colder seasons. In the future, we will use satellite observations of surface temperature (Comiso, 2000), calibrated with data from AWS stations on the ice sheets, to model the elevation changes expected from temperature variations, so that elevation changes caused by precipitation variations and ice flow can be evaluated.

ACKNOWLEDGEMENTS

We appreciate very much discussions with Richard Alley and Matt Spencer on their work on densification, the assistance of Waleed Abdalati and Konrad Steffen in providing and helping us interpreting the AWS data, the cooperation of David Bromwich in providing the precipitation modeling results, and help of Weili Wang in calculating the temperature profiles.

REFERENCES

Comiso, J. C., Variability and trends in Antarctic surface temperatures from in situ and satellite infrared measurements, *J. Climate, 13,* 1674-1696, 2000.

Davis, C. H., C. A. Kluever, and B. J. Haines, Elevation Change of the Southern Greenland Ice Sheet, Science, 279, 2086-2088, 1998.

Hamilton, G. S. and I. M. Whillans, Point Measurements of Mass Balance of the Greenland Ice Sheet using Precision Vertical Global Positioning System (GPS) Surveys, J. Geophys. Res. 105, B7, 16,295-16,301, 2000.

Hvidberg, C. S., K. Keller, N. S. Gundestrup, C. C. Tscherning, and R. Forsberg, Mass Balance and Surface Movement of the Greenland Ice Sheet at Summit, Central Greenland, Geophys. Res. Let. 24, 18, 2307-2310, 1997.

Koerner, 1971, A Stratigraphic Method of Determining the Snow Accumulation Rate at Plateau Station, Antarctica, and Application to South Pole-Queen Maud Land Traverse 2, 1965-1966, AGU Antarctic Research Series, 16, 225-238, Wash. D.C. 1971.

Shepherd A., D. J. Wingham, J. A. D. Mansley, H. F. J. Corr, Inland Thinning of Pine Island Glacier, West Antarctica, Science 291, 862-864, 2001.

Zwally, H. J., A. C. Brenner, and H. Cornejo, Surface Elevation Changes in West Antarctica from Satellite Radar Altimetry: Mass Balance Implications, Annals of Glac, submitted.

FIGURE CAPTIONS

Figure 1. Variations of surface air temperature, accumulation rate and snow surface height at Summit of Greenland ice sheet over the period of April 1992 – April 1999. The temperature data were compiled from AWS and passive microwave measurements by Shuman and others (1999). Accumulation rates are from atmospheric (P-E) modeling results from Bromwich (in press) normalized to the mean accumulation rate at summit, and from AWS sonic measurements of surface height by Steffen and others (1999). Surface elevation time series is derived from ERS1-2 satellite radar altimeter measurements with multivariate linear and seasonal sinusoidal fit.

Figure 2. The velocity components contributing to surface elevation change at a given location are accumulation, ablation, firn compression, and the vertical motion due to ice flow.

Figure 3. Field and laboratory experiments of ice deformation and ice-grain growth show that both (a) activation energy, E, and (b) the rate "constant" K_0 are strong functions of temperature. E(T) data are obtained from, and K(T) values are derived from, Jacka and Li (1994).

Figure 4a. Variations of firn temperature calculated at several depths above 15 m for the summit of Greenland region during April, 1992-April, 1999.

Figure 4b. Interannual variations of summer mean firn temperatures (Jun.-Aug.) at several depths above 15 m in Summit of Greenland region during April, 1992-April, 1999. The trend in surface summer temperature is + 0.3° C a^{-1}, and the trend in mean annual temperature is + 0.4° C a^{-1}.

Figure 5. Modeled steady state seasonal variations of surface elevation for Summit of Greenland (a, b) together with corresponding density changes (c). The variations are driven by surface air temperature with a regular annual cycle with amplitude 19° and mean –30 °C at constant accumulation rate of 250 kg m^{-2} a^{-1}. The seasonal variation in surface elevation is 20 cm, but the seasonal variation in the height of the initial surface decreased quickly as in is buried by new accumulation. The seasonal variation in density is about 0.08, which decreases with depth.

Figure 6. Comparison of modeled and observed interannual changes of the snow surface elevation between 1992 and 1999 at Summit of Greenland.

Figure 7. Modeled elevation change caused by observed temperature variations with constant accumulation (a) and caused by observed/modeled accumulation variations with a seasonal variation in temperature without interannual variations.

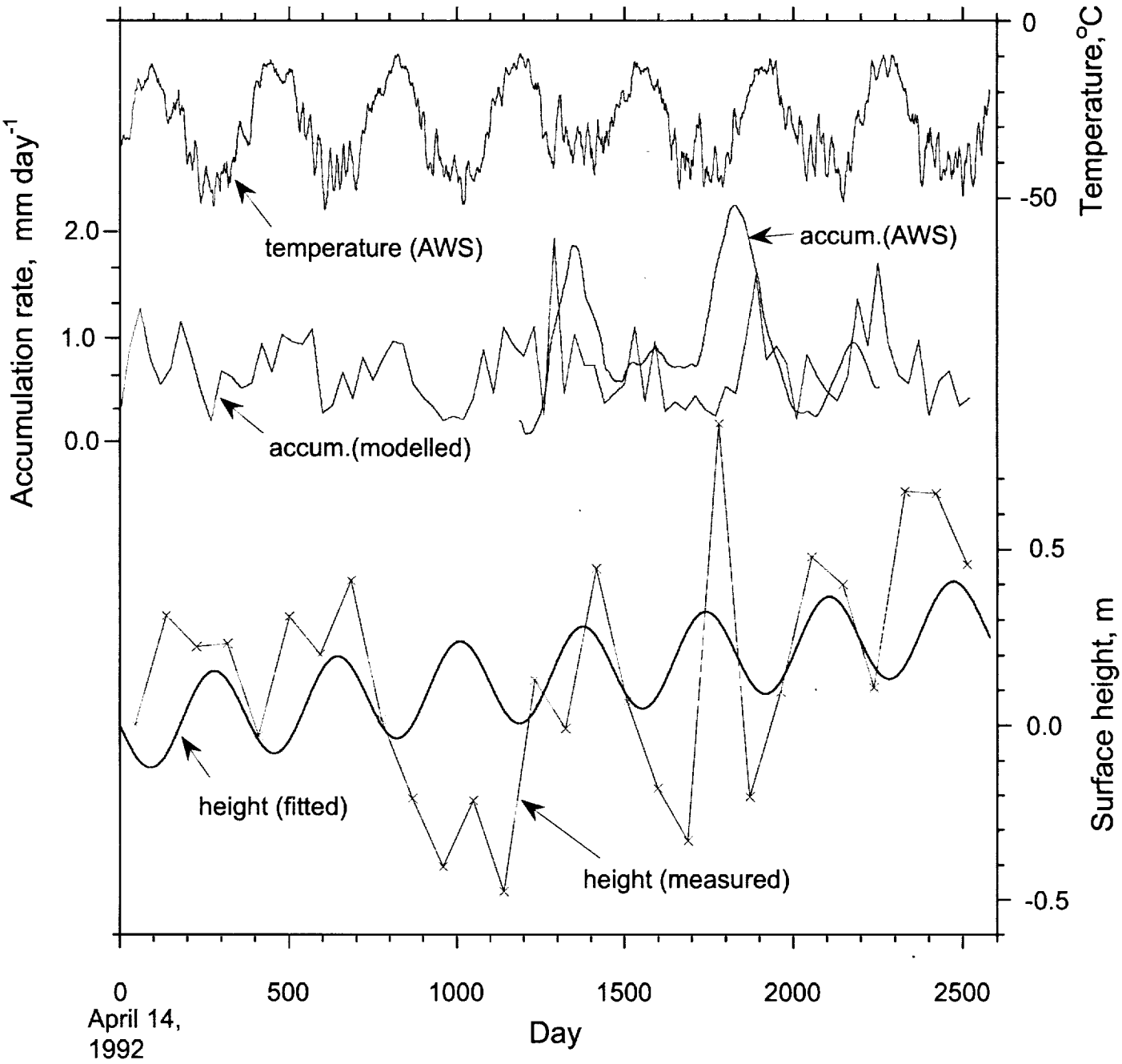
Accumulation rate, mm day^{-1}
2.0
1.0
0.0
0
-50
Temperature,°C
temperature (AWS)
accum.(AWS)
accum.(modelled)
0.5
0.0
-0.5
Surface height, m
height (fitted)
height (measured)
0
500
1000
1500
2000
2500
April 14, 1992
Day

Fig. 1

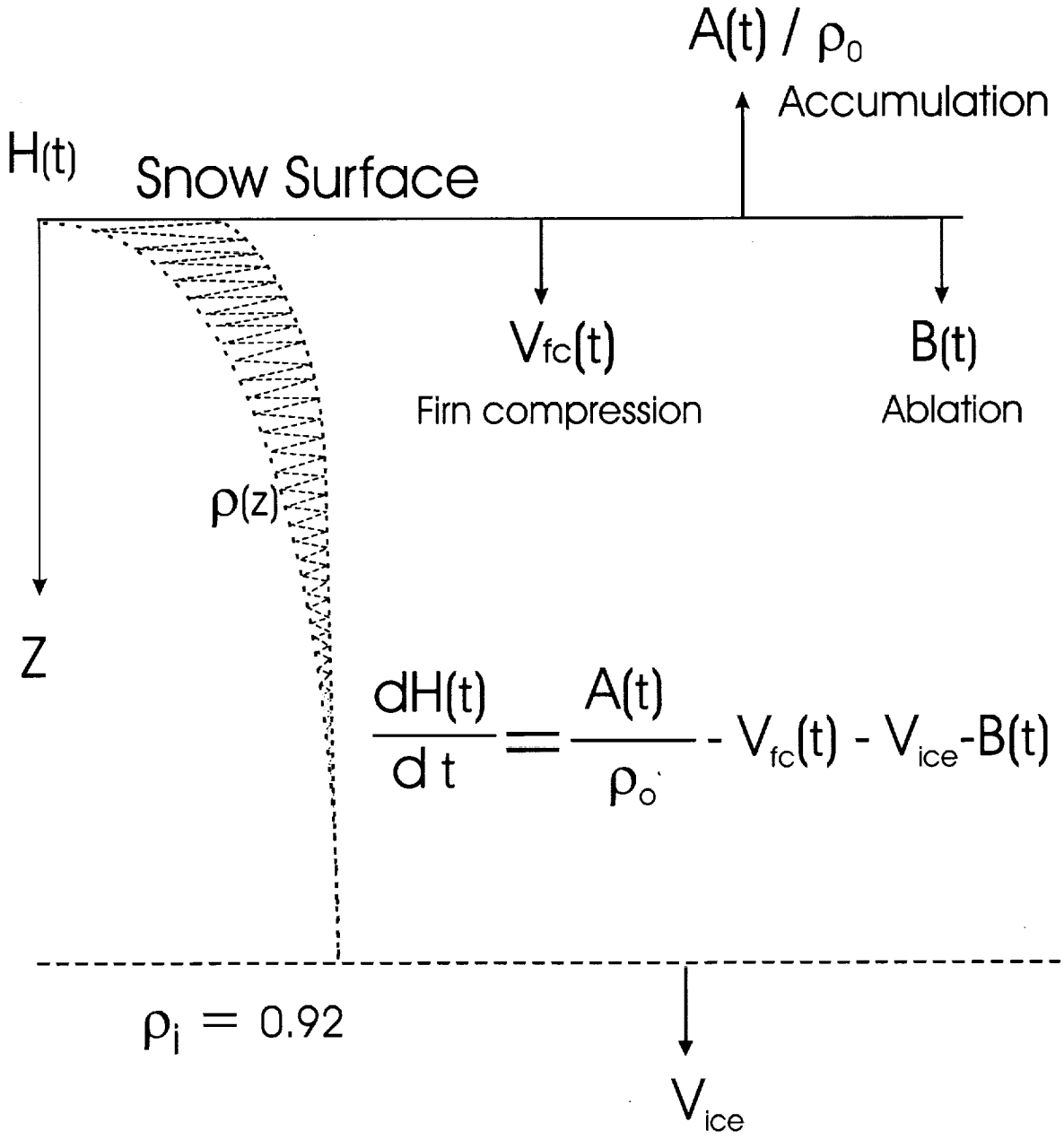
A(t) / ρ0
Accumulation
H(t)
Snow Surface
Vfc(t)
Firn compression
B(t)
Ablation
ρ(z)
Z
dH(t)/dt = A(t)/ρo - Vfc(t) - Vice-B(t)
ρi = 0.92
Vice

Fig. 2

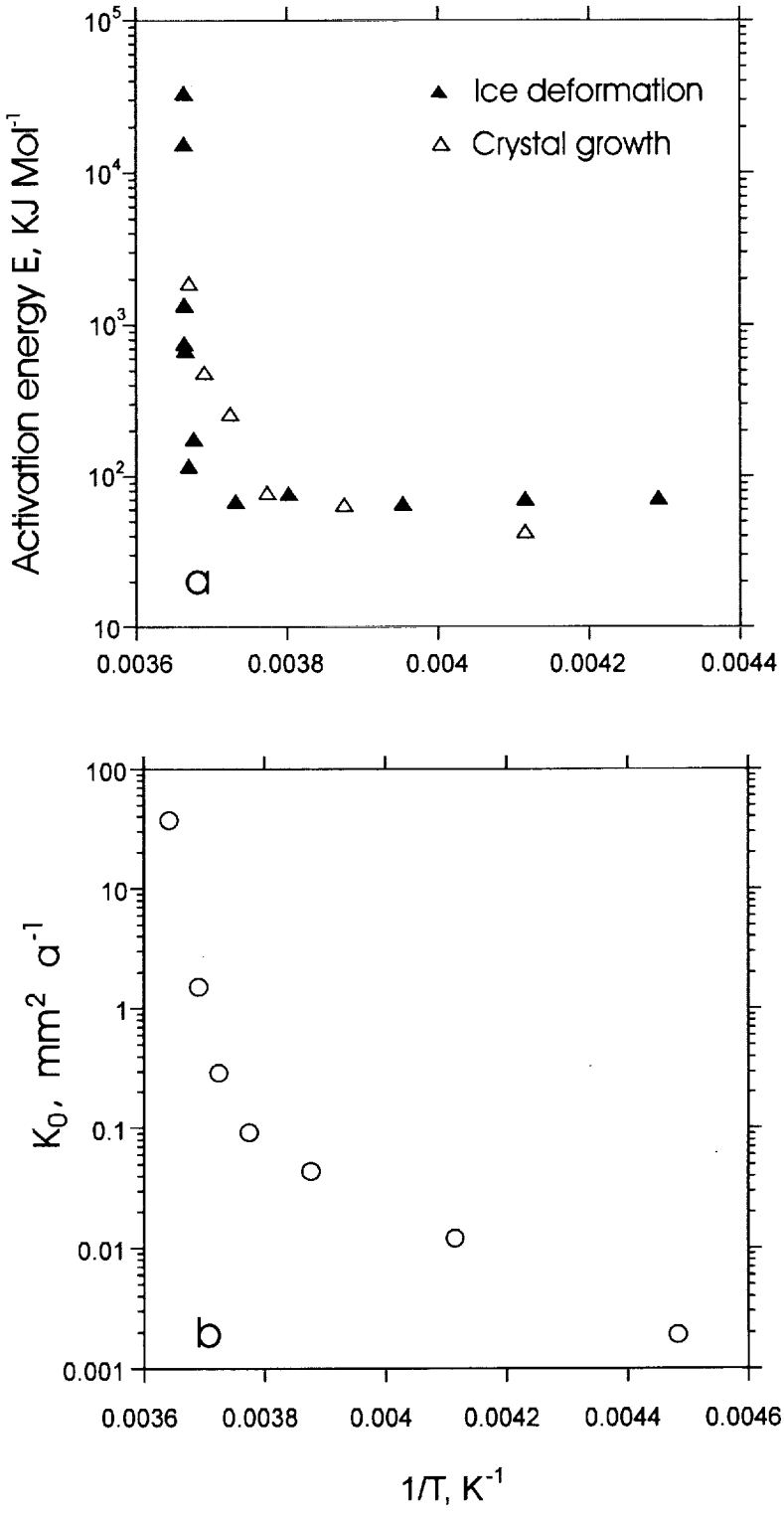
Activation energy E, KJ Mol^{-1}
10^5
10^4
10^3
10^2
10
Ice deformation
Crystal growth
a
0.0036
0.0038
0.004
0.0042
0.0044
K_0, mm^2 a^{-1}
100
10
1
0.1
0.01
0.001
b
0.0036
0.0038
0.004
0.0042
0.0044
0.0046
1/T, K^{-1}

Fig. 3

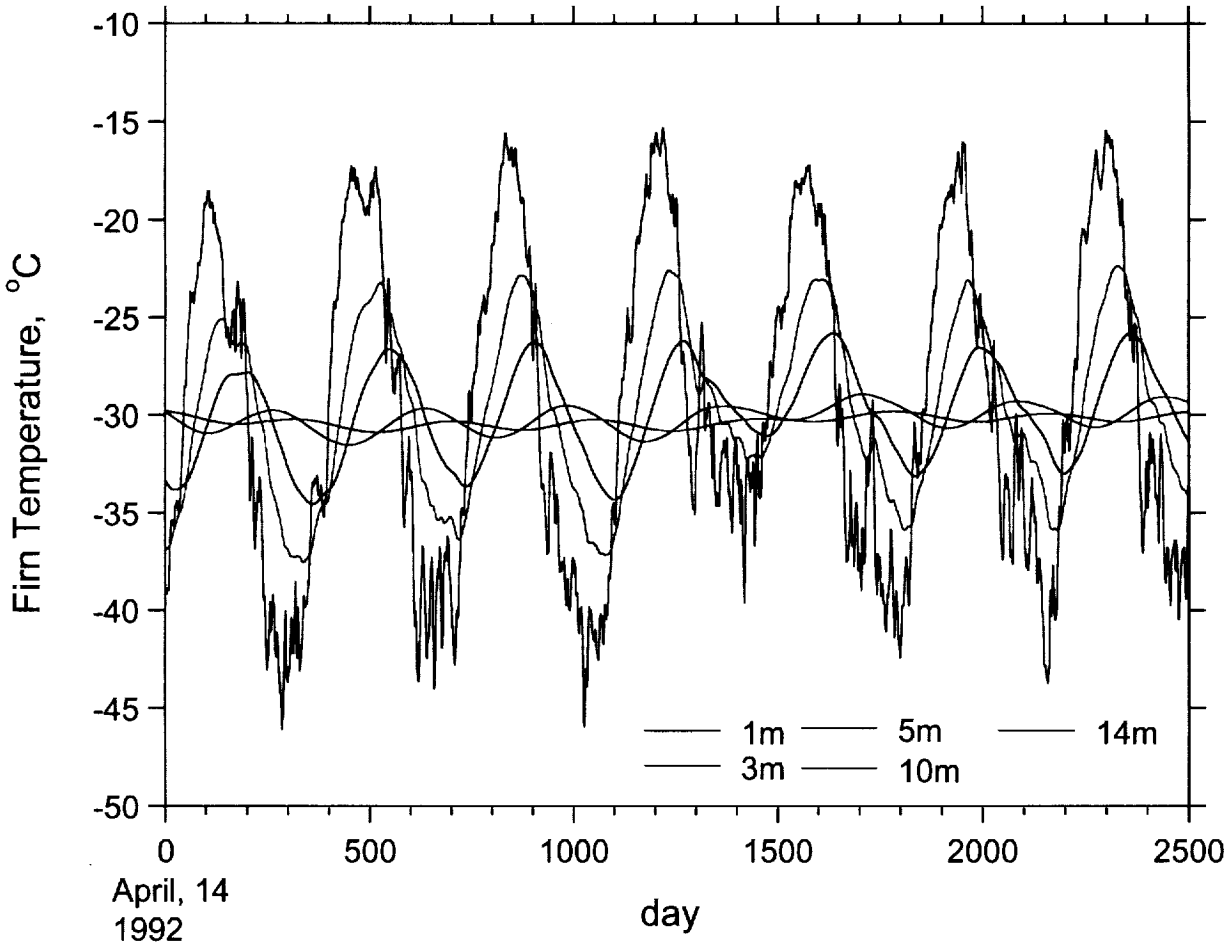
-10
-15
-20
-25
-30
-35
-40
-45
-50
Firn Temperature, °C
1m
3m
5m
10m
14m
0
500
1000
1500
2000
2500
April, 14
1992
day

Fig. 4a

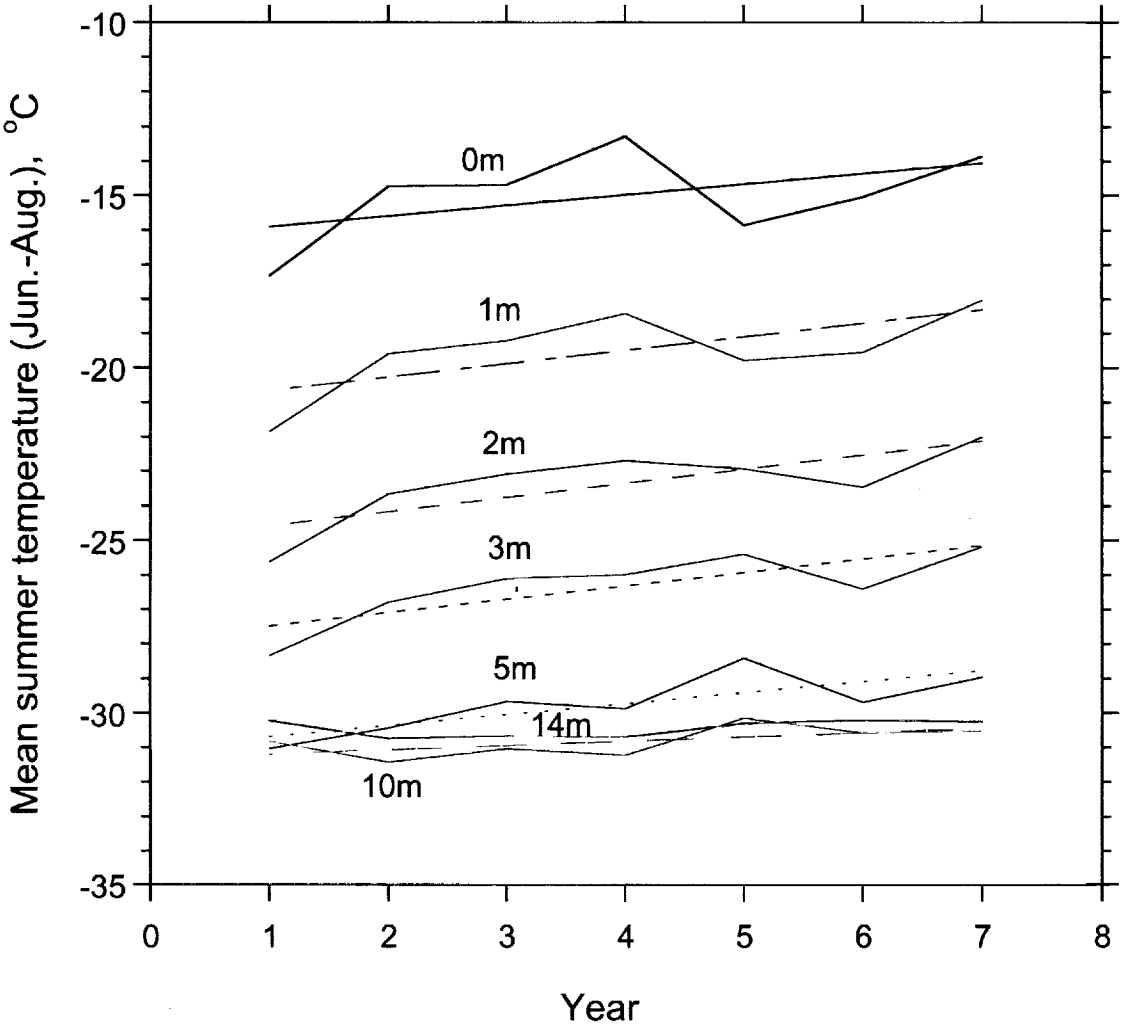
Mean summer temperature (Jun.-Aug.), °C
-10
-15
-20
-25
-30
-35
0
1
2
3
4
5
6
7
8
Year
0m
1m
2m
3m
5m
14m
10m

Fig. 4b

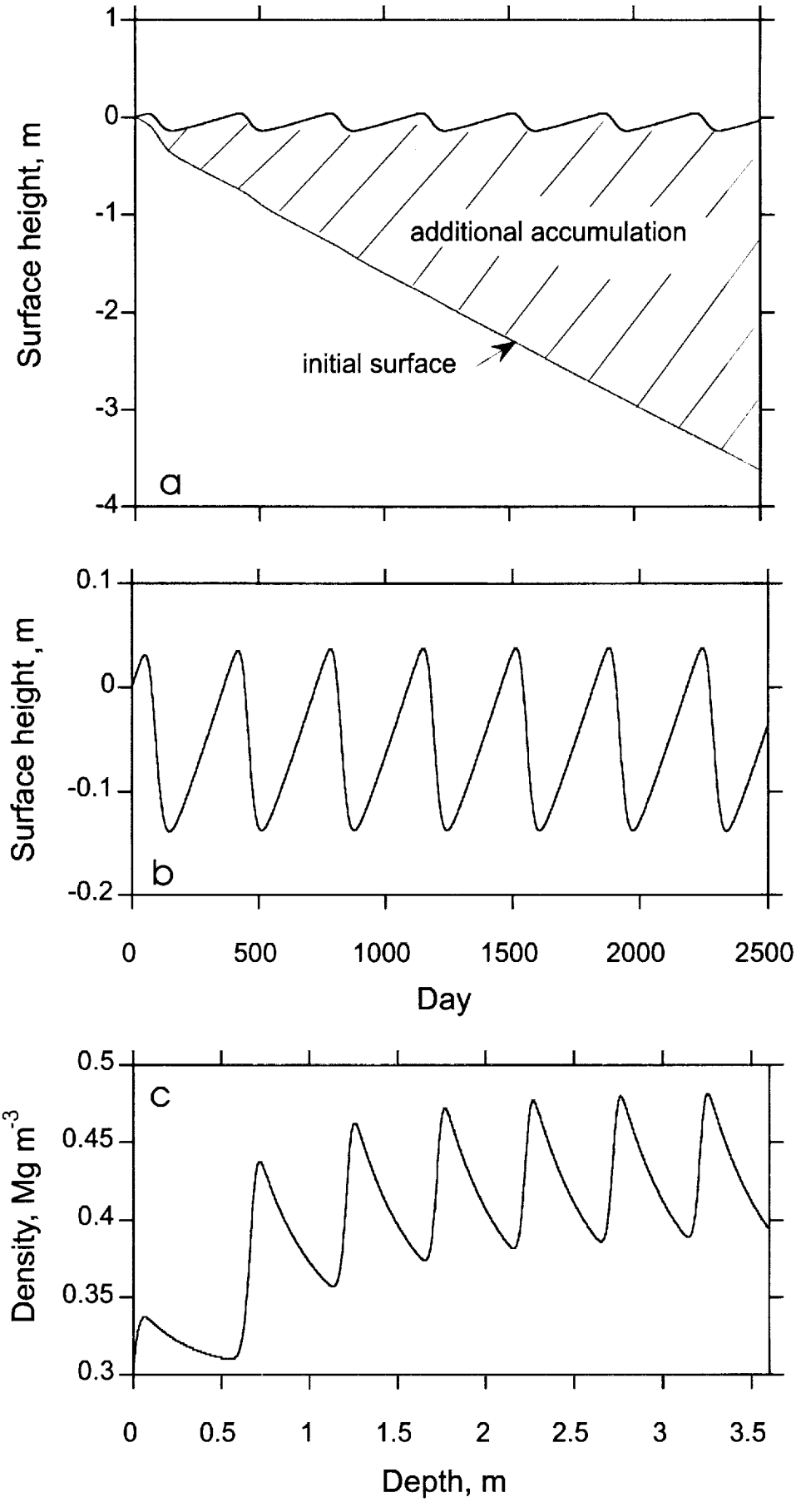
Surface height, m
1
0
-1
-2
-3
-4
additional accumulation
initial surface
a
Surface height, m
0.1
0
-0.1
-0.2
b
0
500
1000
1500
2000
2500
Day
Density, Mg m-3
0.5
0.45
0.4
0.35
0.3
c
0
0.5
1
1.5
2
2.5
3
3.5
Depth, m

Fig. 5

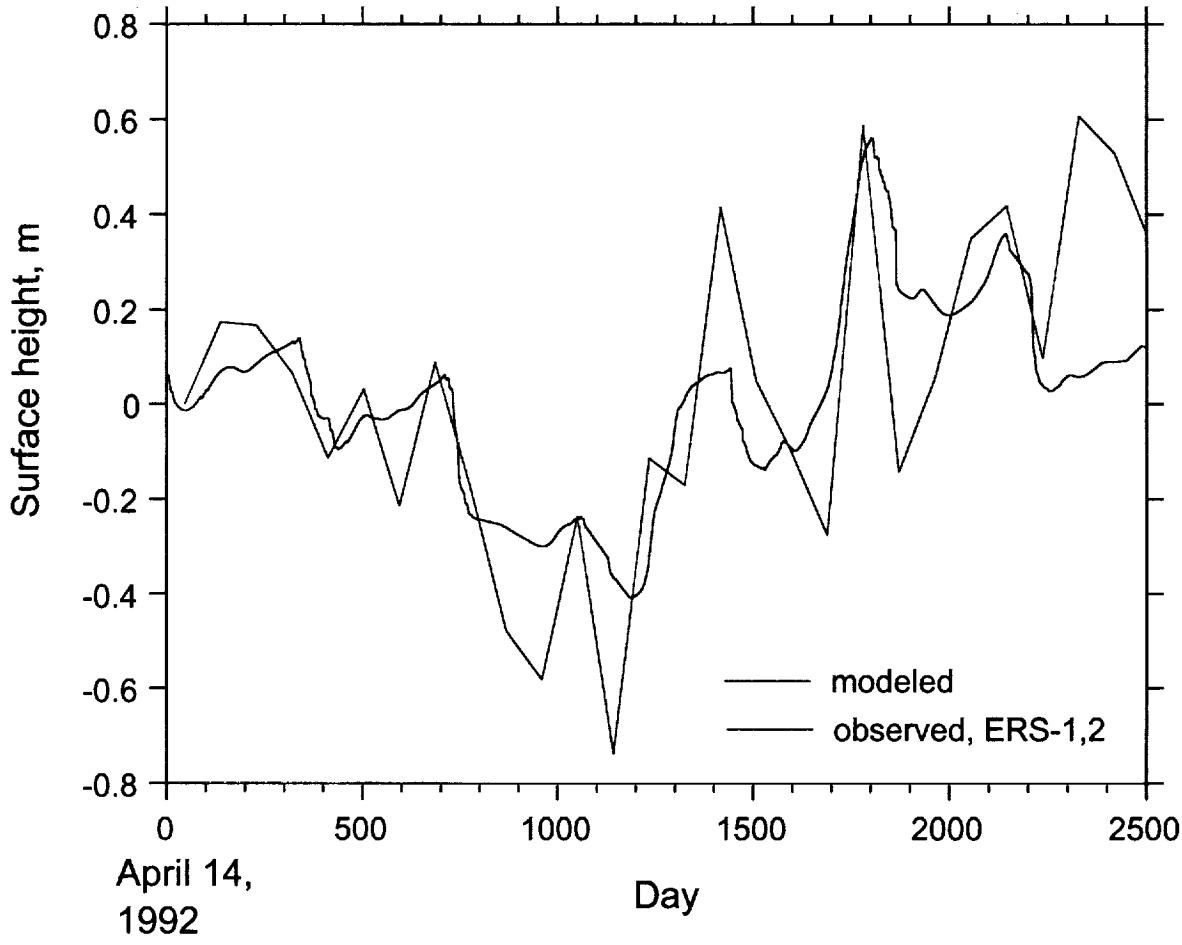
0.8
0.6
0.4
0.2
0
-0.2
-0.4
-0.6
-0.8
Surface height, m
0
500
1000
1500
2000
2500
April 14,
1992
Day
modeled
observed, ERS-1,2

Fig. 6

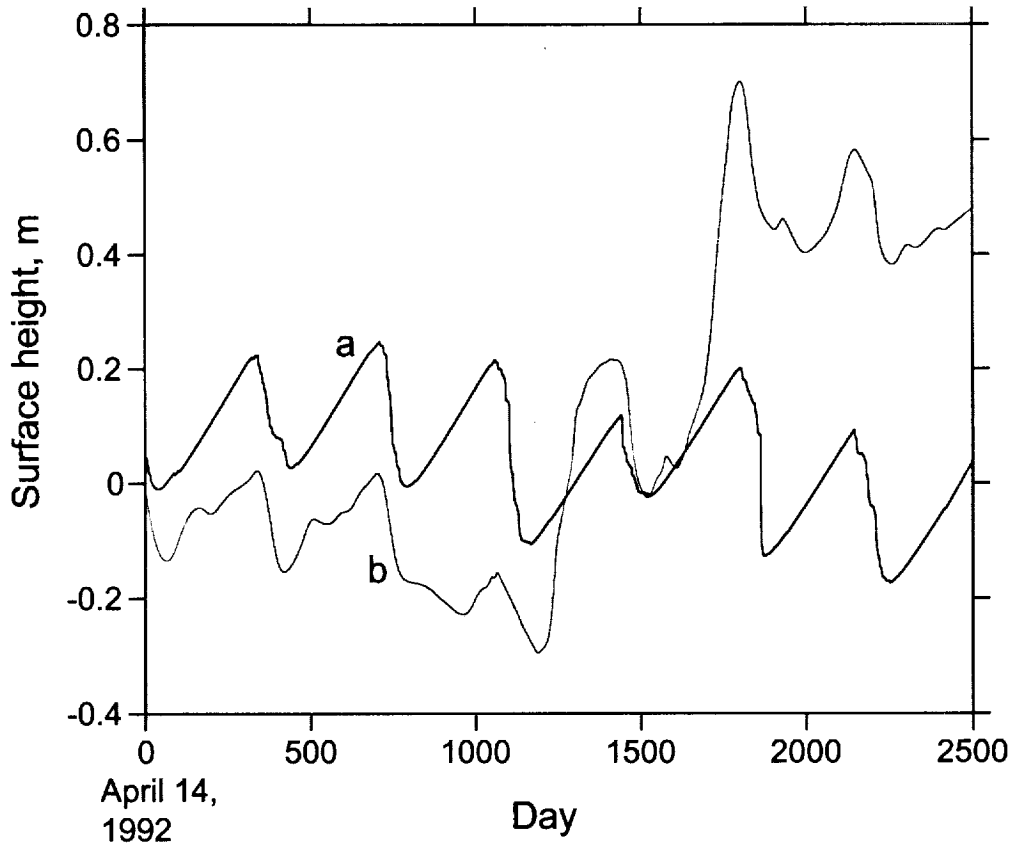
0.8
0.6
0.4
0.2
0
-0.2
-0.4
Surface height, m
a
b
0
500
1000
1500
2000
2500
April 14,
1992
Day

Fig. 7

POPULAR SUMMARY
HJZ, August 16, 2001

Seasonal and Interannual Variations of Ice Sheet Surface Elevation at the Summit of Greenland: Observed and Modeled

H. Jay Zwally and Li Jun

A new model of ice-sheet firn densification shows that there is a seasonal cycle in the rate of densification that causes a seasonal cycle in the surface elevation. This seasonal cycle explains the seasonal cycle observed in satellite radar altimeter data. Observed elevation variations are derived from ERS-1 and ERS-2 radar altimeter data for the period between April 1992 and April 1999. The amplitude of the seasonal elevation cycle is 0.25 m peak-to-peak, with a maximum in winter and a minimum in summer. Inter-annually, the elevation decreases to a minimum in 1995, followed by an increase to 1999, with an overall average increase of 4.2 cm a^{-1} for 1992 to 1999. Our densification formulation uses an initial field-density profile, the AWS surface temperature record, and a temperature-dependent constitutive relation for the densification that is based on laboratory measurements of crystal growth rates. Summer temperatures are most important, because of the strong non-linear dependence on temperature. Much of firn densification and consequent surface lowering occurs within about three months of the summer season, followed by a surface build-up from snow accumulation until spring. Modeled interannual changes of the surface elevation are in good agreement with the altimeter observations. In the model, the surface elevation decreases about 20 cm over the seven years due to more compaction driven by increasing summer temperatures. The minimum elevation in 1995 is driven mainly by a temporary accumulation decrease and secondarily by warmer temperatures. However, the overall elevation increase over the seven years is dominated by the accumulation increase in the later years.